

# Revised Integration Methods in a Galerkin BoR Procedure

David R. Ingham

**Abstract**—Several relatively simple numerical changes improve the speed and accuracy of the early Mautz and Harrington discretization procedure for boundary element method calculations of scattering from axially symmetric bodies. This method is still in common use in programs such as CICERO and GRMBOR. For a fixed set of geometry points, changes in the azimuthal ( $\phi$ ) integration reduce computer time, especially when lossy materials are involved. Changes in the integration along the generating curve ( $t$ ) improve accuracy. The most interesting of these is the use of the equal area rule from parallel wire modeling of solid surfaces to answer the old question of the optimal constant for dealing with an integrable singularity in some of the  $t$  integrals. Some of these changes are applicable to a variety of integral equations and boundary conditions. Most of them can be implemented with little programming effort. Tests are shown for difficult cases involving spheres, and Mie series calculations are used for comparison.

## I. INTRODUCTION

THE old Mautz and Harrington method of reducing integral equations to matrix equations in body of revolution (BoR) scattering [Mautz 1969, 1977] is still in use [Rogers 1989, 1990], though newer procedures have been developed by others [Govind 1978], [Kishk 1992], [Goggans 1992] for example, and by the same workers [Mautz 1982 Mai, 1982 December]. The newer procedures handle the short distance singularity more carefully while the 1976 procedure is simpler and seems to have robustness and efficiency from its use of Galerkin's Method. Its simplicity has allowed it to be used in general computer programs that might otherwise be prohibitively awkward [Rogers 1990]. The McDonnell Douglas implementations such as CICERO [Mitschang 1984 August, 1984 November], [Putnam 1984] exploit the advantages of the early algorithm by being symmetrical, compact, fast and general.

Though singularity removal is necessary for some problems such as tapered coatings, one can argue that the most efficient solution to a symmetrical

David R. Ingham is with Information Communications Architects, Sunnyvale Calif.

Portions of this work were done while David Ingham was with the Lockheed Missiles & Space Company, Palo Alto, CA

problem must be symmetrical itself. EFIE CICERO is almost completely symmetrical with respect to the exchange of the incident and scattered plane waves (and with respect to the exchange of  $\epsilon$  and  $\mu$ ).

The McDonnell Douglas programs have unusually good efficiency in terms of giving reasonable accuracy for small numbers of basis functions and small computer time, but they do not converge quickly enough, for some purposes, when the sampling density is increased. On examining the formalism, it seemed that there might be weakness in the numerical integration in the  $t$  direction. The computer program CIX2 (also called DICIC or CIXFIX) is a version of CICERO with several changes to the numerical integrations by which it calculates the MoM matrix elements.

The first changes resulted in increased speed for cases with wide ranges of refractive index, rather than in increased accuracy. The version with only changes of this type was called CIX1. Additional changes verified the supposition that the  $t$  integrations limited the accuracy. The original scheme was simple and fast but did not give high accuracy. On the other hand the more elaborate methods of programs such as DBR [Glisson 1979, 1980] and JED (a Lockheed Missiles and Space Company (LMSC) program using the later Harrington and Mautz method) tend to be specialized to their basis and testing functions. We wished to preserve CICERO's triangle basis functions and Galerkin's method that appear to account for its efficiency, and to stay within the framework of its geometry description.

Each change was tested for the conducting sphere, for which a good bench mark is available [Smith-Subbarao 1987]. A few final variations were compared also against coated spheres and against experimental data.

## II. THE SIGNIFICANT DIFFERENCES

### A. Changes to the $t$ Integration

1) The basis and testing functions of this method are triangles (with some lone half triangles at junctions). When these are differentiated, they become double pulses. The intervals between adjacent pairs of the user's geometry points are usually called segments. Each half triangle covers two segments. The integration sampling points of the original procedure are the centers of the segments. In CIX2 the segments are

divided into "subintervals" for numerical integration, whenever the distance between them at  $\phi = 0$ , ( $|t - t'| = \sqrt{(z-z')^2 + (\rho-\rho')^2}$ ) is smaller than the wave length ( $\mathcal{L}$  operator) or half the wave length ( $\mathcal{S}$  operator). This improves accuracy, at the expense of fill time. The number of these subintervals depends on the distance. It is two for  $|t-t'| > \lambda/2$ , three for  $|t-t'| > \delta$  and five for  $|t-t'| \leq \delta$  ( $\mathcal{L}$  operator), and two for  $|t-t'| > \delta$  and three for  $|t-t'| \leq \delta$  ( $\mathcal{S}$  operator), where  $\delta$  is the average of the source and field segment widths.

2) The treatment of the logarithmic singularity in the  $t$  integrations contributing to the  $\mathcal{L}$  operator contained a small error, which was corrected. This might not be regarded as an error at the time the method was first proposed, but it has slowed the method's convergence as computer hardware has improved.

These programs do not subtract out this integrable singularity. The  $t$  integration proceeds with constant steps and weights except that when the source interval is the same as the field interval, the value of zero for  $|t-t'|$  is replaced by  $1/4$  of the segment width. The original explanation for this procedure was that it corresponds to using a cylinder equivalent to a strip. Another interpretation is that it subdivides the interval and samples each half at its center. This is not the best choice. The imaginary parts of the integrands are smooth. The real parts are concave upward in each interval (for small  $|t-t'|$ ). So integrating by intervals sampled at their centers always gives estimates of the contribution to the integral from the neighborhood of the singularity that are too small.

The new algorithm corrects this systematic error by using the appropriate equivalence between a cylinder and a strip. This is the same equivalence as the equal area rule for parallel wire modeling of surfaces. The  $\delta/4$  is accordingly changed to  $\delta/(2\pi)$ . Test numerical integrations verify this new value. (See Part IV.)

[Kishk 1989] and Shafai found that sampling the dielectric side of an interface more densely than the vacuum side improves the efficiency, but the current author only became aware of his work through the editors of this journal.

### B. Changes to the $\phi$ Integration

Gauss Legendre quadrature is not an obvious choice for a periodic function (with no ends). Yet, it deals well with the spike in the integrand centered at  $\phi=0$ , because the integration points bunch up near the limits of integration.

1) The number of  $\phi$  integration points (NGAUSS) is different for each region. This avoids using unnecessary points for low refractive index materials, when there are dense materials in the problem. In particular, it avoids using an unnecessarily large value of NGAUSS while computing the submatrices for the outside free space. This can be the most time-consuming part of this program. Making the  $t$  sampling density depend on the dielectric constant has previously been shown to improve efficiency [Kishk 1989].

2) The Green's Function integrals terminate at large distance in lossy materials when the  $e^{-jkz}$  factor is less than a small constant value. (It made little difference whether this number was  $10^{-7}$  or  $10^{-4}$ .) This avoids calculating negligible terms. This test is so effective for lossy high refractive index materials that it seems preferable, for these cases, to singularity removal, which results in an integral that cannot be truncated. The original version of CICX2, running on a scalar computer, jumped out of the  $\phi$  integration loop. To optimize the program for a vector computer, it was necessary to find the number of  $\phi$  steps needed before entering that loop. The program searches the table of integration abscissas for an approximate match to the required number of skin depths.

3) The Gauss Legendre weights and abscissas used are half of those for an integration from zero to  $2\pi$  instead of those for zero to  $\pi$ . In other words the call to the subroutine GAUSS has the parameters  $2$  NGAUSS and  $2\pi$  instead of NGAUSS and  $\pi$ . This avoids unnecessarily bunching the integration points near  $\phi = \pi$  where the integrand is well behaved. We are integrating even periodic functions from zero to  $2\pi$ . The old way is to divide each integral into two equal parts, one from zero to  $\pi$  and one from  $\pi$  to  $2\pi$ , and then to use Gaussian quadrature on one of these equal parts. The new method uses Gaussian quadrature on the interval from zero to  $2\pi$  but only evaluates one of each pair of equal samples.

4) NGAUSS now depends on the absolute value of the refractive index rather than on the real part only. The derivatives of the integrand depend on the imaginary part of  $n$  as well as on the real part. This should improve the accuracy for very lossy materials. The time cost is small because of 2) above.

The formula for NGAUSS used here is the nearest integer to  $4n\rho_{\max}/\lambda_0 + 2.5$ , or 12, whichever is larger. Here  $n$  is the absolute value of the refractive index,  $\rho_{\max}$  is the largest value of the radius in the current region and  $\lambda_0$  is the free space wave length. The formula for NGAUSS in old CICERO is the largest integer less than  $2(n\rho)_{\max}/\lambda_0 + 1.5$ , or 8, whichever is larger. Here  $n$  is the real part of the

refractive index,  $\rho$  is the radius,  $(n\rho)_{\max}$  is the largest value of  $n\rho$  in any region and  $\lambda_0$  is the free space wave length. NGAUSS was increased, as needed to compensate for the less smooth form of the integrand resulting from the smaller values of  $|t-t'|$ , when subintervals are used.

5) The  $\phi$  integrals at longer  $|t-t'|$ , where no subintervals are used, are done on a smaller number of equally spaced  $\phi$  values with equal weights. This is the obvious choice for a well behaved periodic integrand.

### III. TEST CASES

The data shown were computed with 64 bit precision. See section IV for comments on arithmetic precision.

#### A. Conducting Sphere

Figure 1 is a logarithmic plot of the back scatter cross sections calculated by the new and old versions of CICERO and by a Mie series calculation for a conducting sphere with a one meter radius. Both CICERO calculations are for the same segmentation of the sphere. There are about ten basis functions

(20 geometry points) per free space wave length at the highest frequency shown.

All three agree well, except that the standard CICERO calculation begins to change rapidly with frequency near the upper end of the frequency range. This behavior is associated with cavity resonances. {The scattering problem could be solved by a McDonnell Douglas variant with the Combined Field Integral Equation [Mitschang 1984 November] [Putnam 1987], but the interest here is in a measure of the numerically generated transparency of the conducting surface that allows the cavity resonances to couple to the exterior field.}

Figure 2 shows more frequency steps in this upper region. The new version shows resonant behavior, but the resonances are localized to certain frequencies with smooth regions between. With the original version, the resonances are broadened by numerical error to the extent that they overlap.

Figure 3 shows the first minimum. Though the number of basis functions per wave length is much larger here than at the higher frequencies calculated, there is a fraction of a dB error in the old CICERO calculation. This is smaller with the new version.

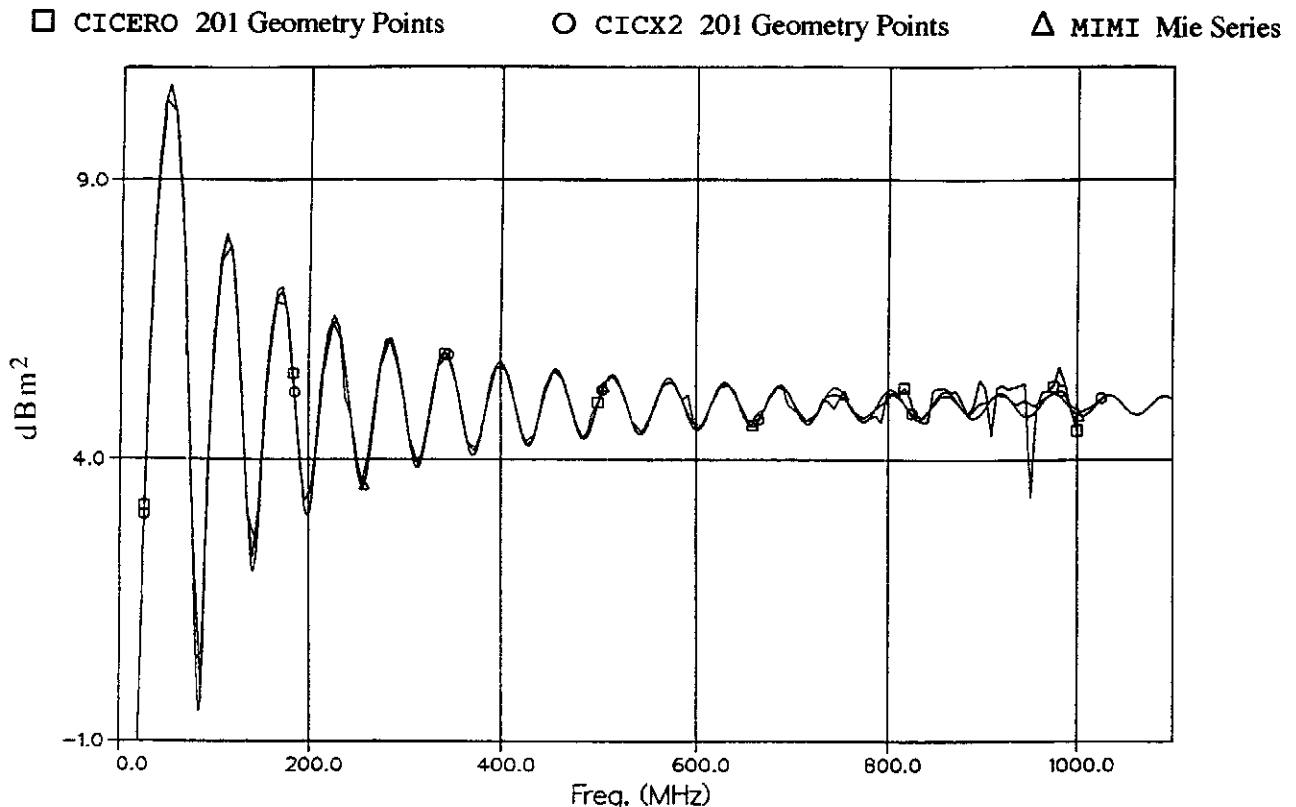


Figure 1: Back-Scatter from a Perfectly Conducting Sphere (1 meter radius) Rayleigh Region to 1 GHz.

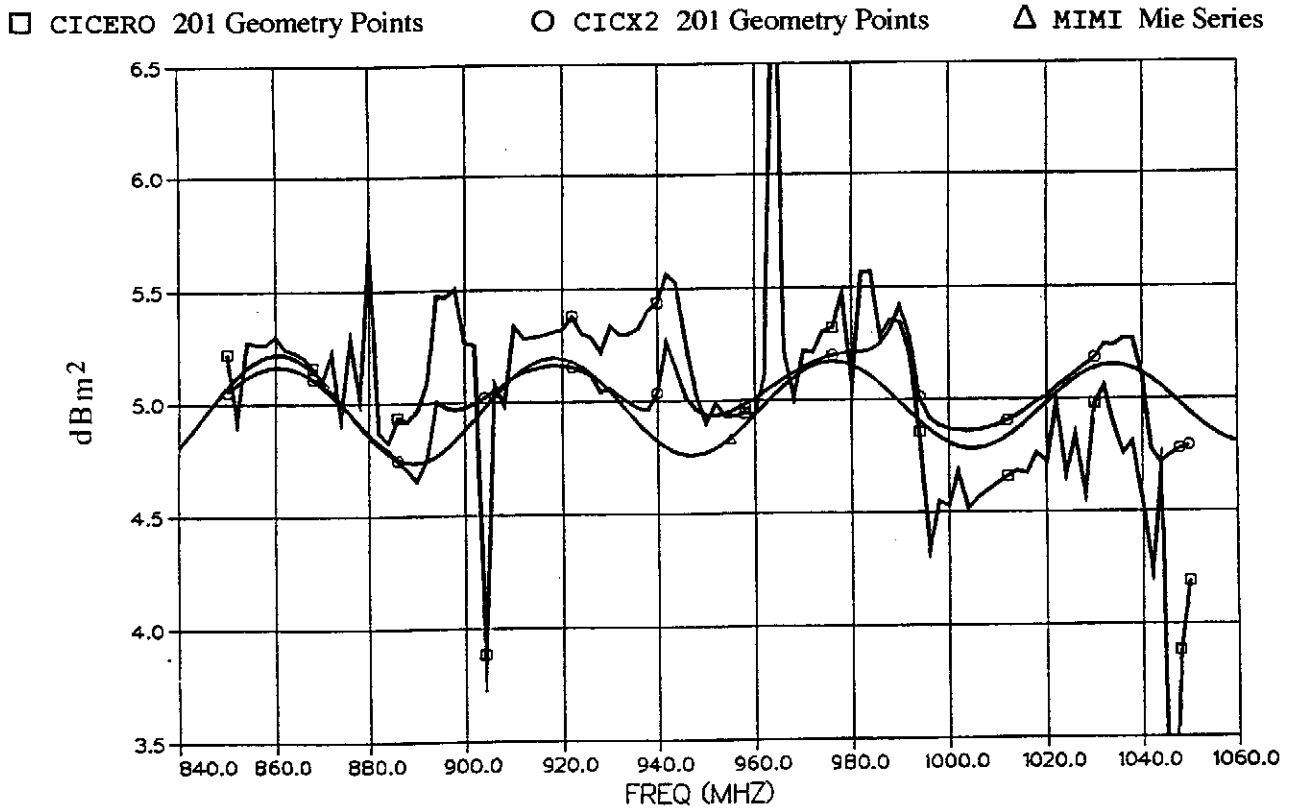


Figure 2: Back-Scatter from a Perfectly Conducting Sphere Region of 1 GHz.

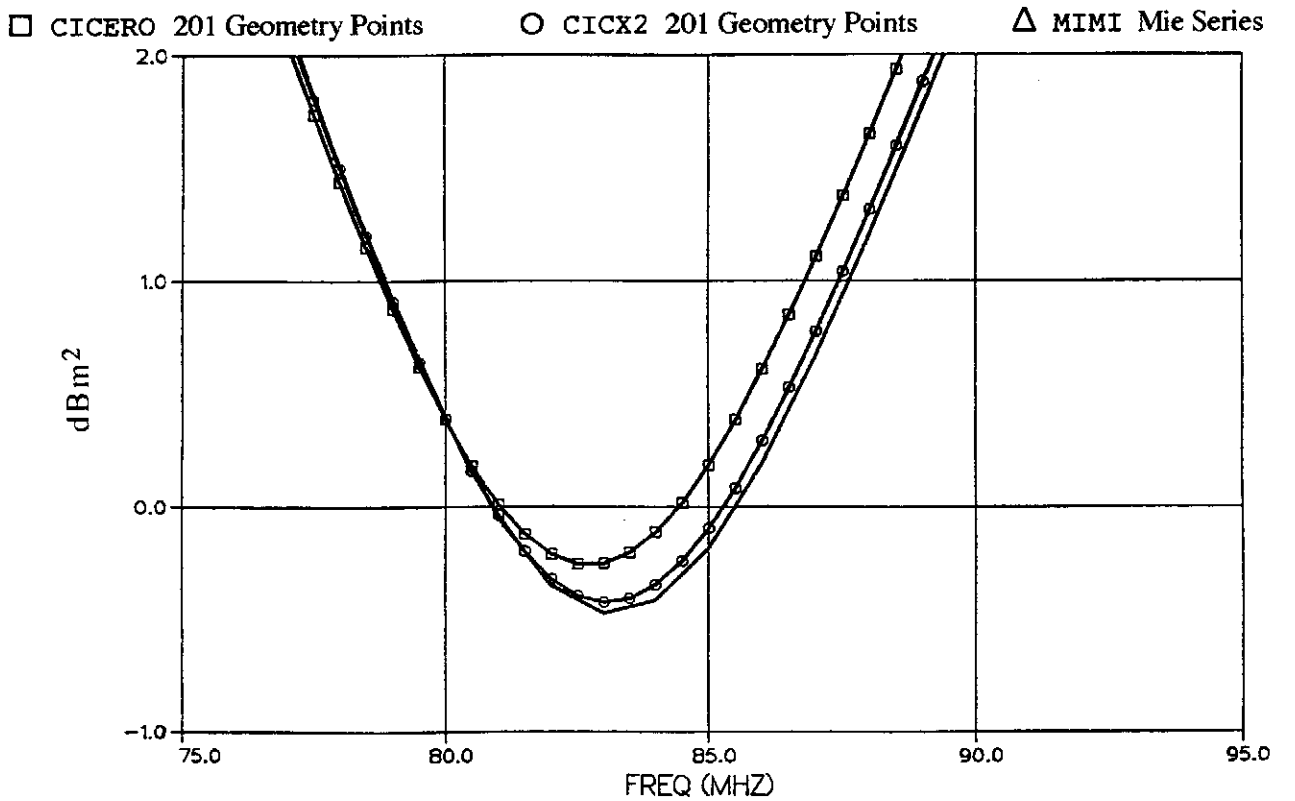


Figure 3: Back-Scatter from a Perfectly Conducting Sphere Region of the First Resonance Minimum

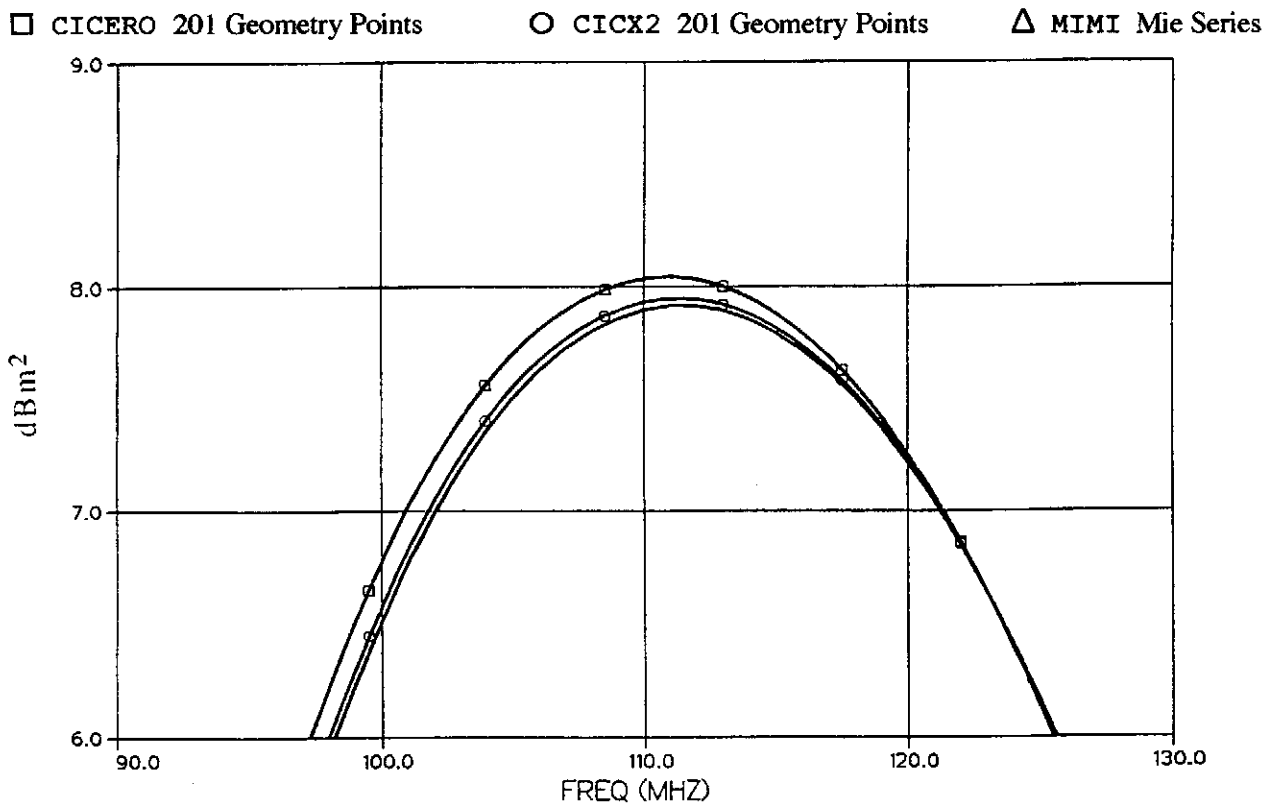


Figure 4: Back-Scatter from a Perfectly Conducting Sphere Region of the Second Resonance Maximum

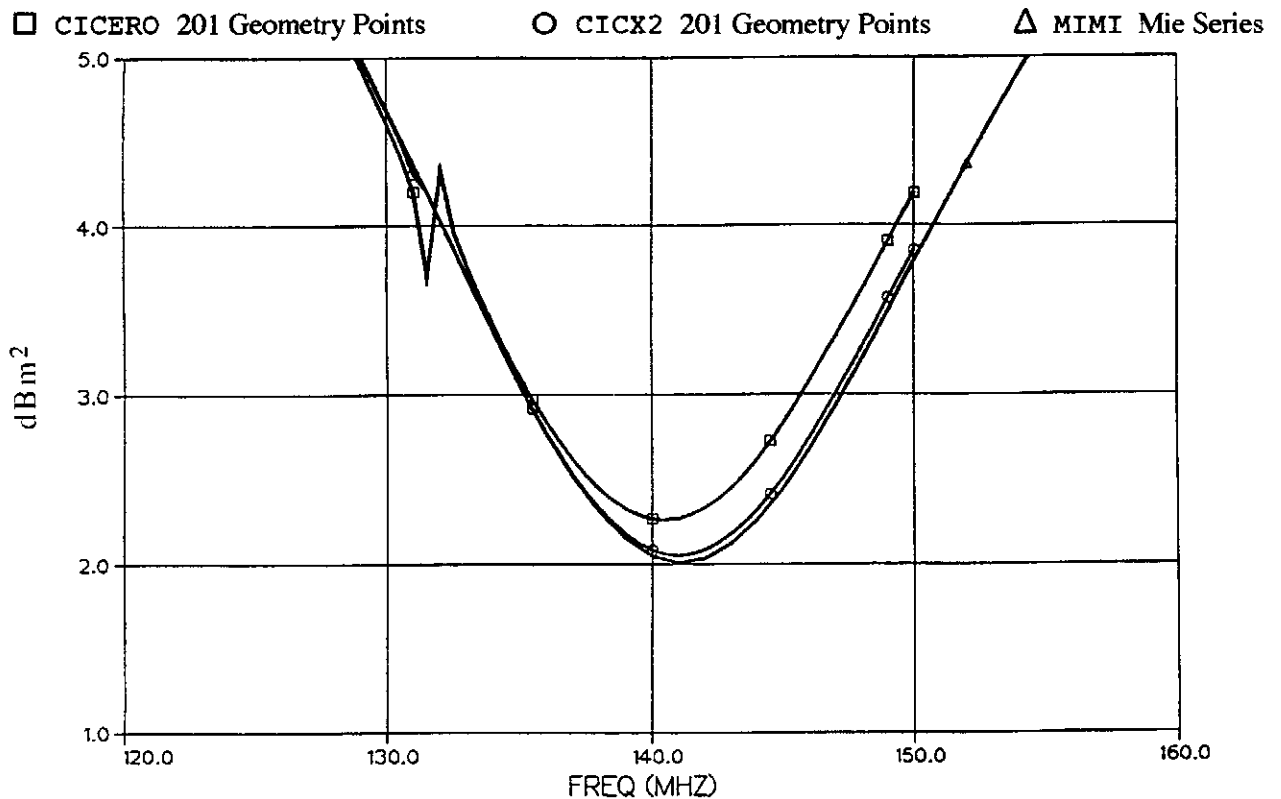


Figure 5: Back-Scatter from a Perfectly Conducting Sphere Region of the Second Resonance Minimum

Figure 4 shows the second maximum with generally the same results. In Figure 5, the region of the second minimum, there is one isolated cavity resonance. This is just visible in this view of the calculation with CICX2 and is more pronounced in that with CICERO.

### B. Vacuum Coated Conducting Sphere

Figure 6 shows a conducting sphere, calculated as a conducting core coated by a dielectric with the  $\epsilon$  and  $\mu$  of free space. Here the old and new versions do about equally well. The only version that does better, here, is a version (labeled L) with more integration steps even for large distance between source and field segments. This result supports James Rogers's use of more than two segments per half triangle. It also suggests that these long distance matrix elements might be an appropriate target for future work.

### C. A Sphere with a Lossy Coating

Figure 7 shows the back scatter cross section of a sphere with a lossy coating. The coating has (relative)  $\epsilon$  about 10 and  $\mu$  about 3. It has both electric and magnetic loss. Its loss and thickness (about 2.5 cm.) give perfect absorption at normal incidence on a flat surface at 500 MHz. In an impedance boundary condition approximation, there is zero back scatter from the coated sphere at the same frequency. The Mie calculation with the program MIMI [Smith-Subbarao 1987] shows that the true cross section is very small at this frequency. On the other hand it comes up rapidly away from 500 MHz., because of the specular reflection. This case is very sensitive to the modeling of the coating properties.

□ CICERO 201 Geometry Points      ○ CICX2 201 Geometry Points      ▲ L Version of CICX2  
 × MIMI Mie Series

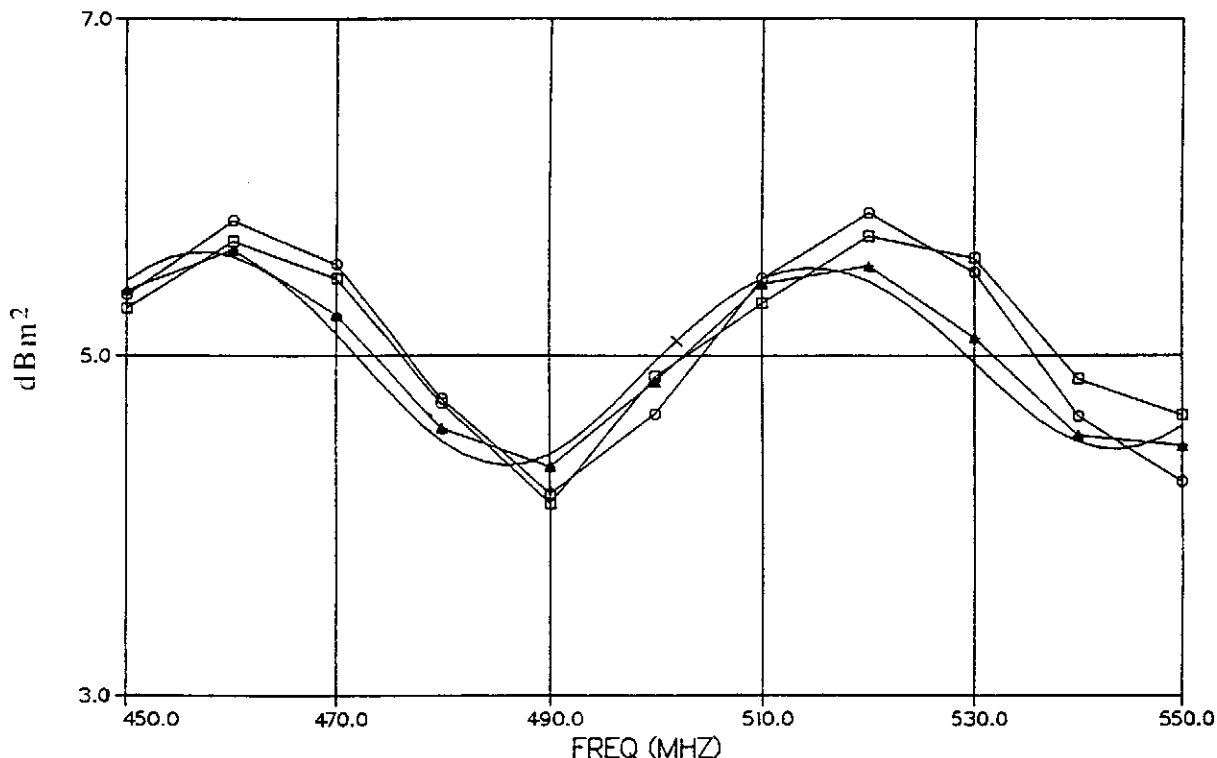


Figure 6: Back-Scatter from a Perfectly Conducting Sphere Calculated as a Coated Sphere

- CICERO 201 Geometry Points: About 10 basis functions per free space wave length
- CICX1 201 Geometry Points. Overlays CICERO Calculation
- △ CICX1 401 Geometry Points: About 20 basis functions per free space wave length
- + CICX1 801 Geometry Points: About 40 basis functions per free space wave length
- × CICX2 201 Geometry Points.      ◇ MIMI Mie Series

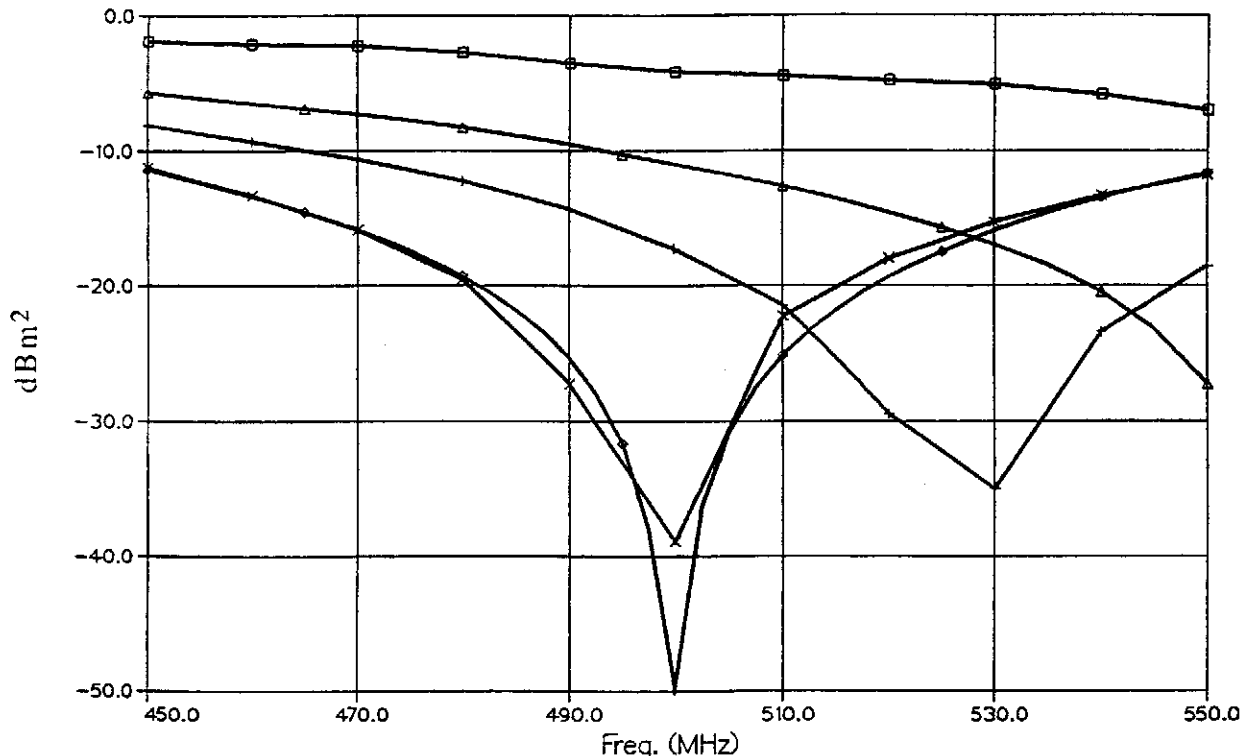


Figure 7: Back-Scatter from a Coated Sphere Outer Radius = 1 Meter, Coating Thickness = 2.2 cm.

The BoR curves shown here are for three different geometry point spacings with the CICX1 version and the coarser spacing with the new CICX2 version. A calculation done at the coarser spacing with the old CICERO is shown to verify that the result is indistinguishable from that with CICX1. Some luck is involved. A version with more integration points for the  $\mathcal{H}$  operator does not do quite so well on the resonant frequency. But there is clearly a large improvement. Other experience also supports the conclusions that CICERO underrepresents the electrical thickness of coatings and that this tendency has been corrected in CICX2. The systematic part of the error was presumably due to the undersampling of the  $1/r$  singularity, though no specific trial has been done to confirm this.

#### D. Sphere Imbedded in a Cylinder

The only case noticed, for which the modifications hurt the accuracy was a conducting sphere enclosed in a cylinder with the  $\epsilon$  and  $\mu$  of free space. Whether this shows any fault in the changes described here is not known.

#### E. Computer Time

Even for equal numbers of basis functions, the computer times are different for the two versions. The CICX2 uses many more  $t$  integration steps at short distances than the old CICERO but conserves on  $\phi$  steps, especially at large distances. It is slower for electrically small perfect conductors and faster for large lossy bodies.

### IV. THE EQUAL AREA RULE AND THE BoR MATRIX ELEMENTS

The  $\phi$  integrals required for the matrix elements are:  $G$ ,  $G_c$  and  $G_s$  for the  $\mathcal{L}$  operator, [Mitschang 1984 November, p. 28] and  $H$ ,  $H_c$  and  $H_s$  for the  $\mathcal{H}$  operator [p.33]. The first three of these contain a factor of  $1/(kr)$ .  $G_s$  also contains a factor of  $\sin(\phi) \sin(n\phi)$  that cancels the singularity at  $\phi=0$ .

The three integrals for the  $\mathcal{H}$  operator nominally contain a factor of  $1/(kr)^3$ . Here one factor of  $1/(kr)$  is

from the Green's function itself, one results from differentiating the green's function (instead of the basis and testing functions as for the  $\mathcal{L}$  operator) and one is merely the result of using the position vector instead of the corresponding unit vector in defining the direction. The magnetic field on a flat sheet of current depends only on the local value of the current, which is included separately. So the contribution of these integrals, for  $t$  and  $t'$  on the same segment and  $\phi$  small, must vanish. The singular parts of the integrals do not contribute, except through roundoff error.

In the original form given by [Mautz 1977, p.9], only one of the three integrals of the  $\mathcal{H}$  operator has the  $1/(kr)^3$  form. Its coefficient explicitly vanishes for the self term, so they avoid this subtraction of large numbers. For the cases tested, changing the numerical precision of these variables or of the whole program between 64 and 32 bits had little effect, but one should suspect them when he/she sees precision dependence with the McDonnell Douglas form.

The two dimensional integrals, then, are all either smooth or of the form  $1/(kr)$ . We integrate in the  $t$  direction by dividing each basis function into segments (and subintervals) and sampling at the center of each interval. Where the source and field intervals are the same, we would get infinity for the  $\phi$  integral, so we further divide the interval into two. At this point the old algorithm again samples each of these half intervals at its center and therefore underestimates the integral. By the mean value theorem, there is some point where we can sample the function and get the right answer, for the real part. If the interval is much smaller than a wave length in the material, then the correct choice of the  $t$  location at which to sample does not depend strongly on the  $e^{-jk_r}$ ,  $\cos(\phi)$  and  $\cos(n\phi)$  factors in the integrands. The contribution of  $|t-t'|$  to  $|r|$  will have died out before these slowly varying functions begin to deviate from unity. As usual, the short range effects can be regarded as electrostatic and magnetostatic.

We need an approximation for the integral, based on sampling the distant intervals at their centers. Such an approximation is in use in electromagnetics. It is commonly called the "equal area rule" [Ludwig 1987]. One statement of this is that the electrostatic energy (and the magnetostatic energy, which has the same form) of a row of circular cylinders most closely approximates that of a plane when the circumference of each cylinder is equal to the spacing between them. This energy can be evaluated by adding the contributions of the charges on the cylinders (assumed

axially symmetrical) to the electric potential on the surface of one of them. It gives the same form as integrating by strips, sampling each but the self term at its center and sampling the self strip at  $\delta/(2\pi)$  from its center. This, is the relevant equivalence between strips and cylinders.

Other values such as  $\delta/8$  [Kishk 1986], [Kishk 1992] and even  $\delta/6$  (rumor) have been tried, but the equivalence of this integral to those in the standard "user" equal area rule has apparently been missed.

### A. Wire Modeling of Surfaces

A wire screen can be modeled as an equivalent circuit between two 377  $\Omega$  transmission lines that model free space [Marcuvitz]. This circuit may have resistive loss, inductance and capacitance. If the screen has no loss, the circuit has no resistance. The inductance and capacitance are measures of the magnetic and electric field energies stored near the mesh. More precisely, of their differences from the field energies in free space.

The group who founded TCI noticed, perhaps during the design of a wire grid Luneburg lens before that company was founded, that the electrical properties of mesh depend on both the magnetic and electric field energies [Andreasen 1962, TCI]. To match a solid metal plate, both field energies must match those of the plate. For crossed wires, one must resort to nonphysical (for wire) negative series inductance to do this, because the wires perpendicular to the current hold charge but have little effect on the magnetic field. If the polarization is known from symmetry, one can use parallel wire. For parallel wire, the electric and magnetic field energies have the same form, as they do for a flat plate. It is necessary only to pick the right spacing to radius ratio to approximate both energies accurately. Of course the spacing must still be small compared to the wave length and to any relevant geometric features of the body, but the method converges much more rapidly if the correct ratio is used. This ratio is  $2\pi$  [Ludwig 1987]. This is heuristically known as the "equal area rule."

Both a wire with uniform current and one with uniform charge have field proportional to  $1/r$ , so each field energy is the integral of  $1/r^2$  over the space outside the wire. In polar coordinates, this is the integral of  $2\pi r / r^2$  from the wire radius  $\rho$  to some distant point  $R$ . This is proportional to  $\log(R/\rho)$ .



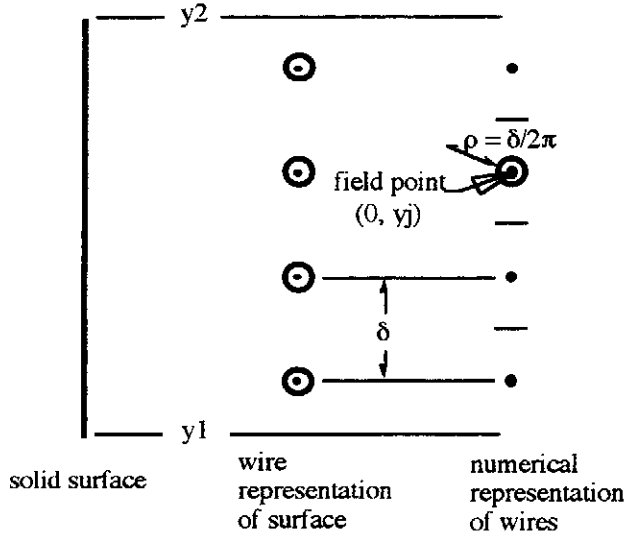


Figure 8: Geometry of the "Equal Area" Approximation to the Electrostatic Potential on a Charged Surface: Short range effects in electrostatics can be approximated by statics.

The equal area rule is a well-established approximation for these field energies, which contain the same singularity as that in the BoR  $\mathcal{L}$  operator integrations. The electric field energy per charge of a (locally) uniformly charged plate is proportional to the scalar potential. This is the integral over the charge of  $1/r$ , as in the  $\mathcal{L}$  operator. The BoR integration points correspond to the wires. This part of the  $\mathcal{L}$  operator can be interpreted as the scalar potential due to a charge distribution. For the self wire, the distance from the line charge used in the  $1/r$  integral is the wire spacing divided by  $2\pi$ . Since the BoR integral has the same form of singularity the distance from the line charge should be taken to be the point spacing divided by  $2\pi$  here also to obtain the same accurate and robust approximation:

$$\int_{x_1}^{x_2} \int_{y_1}^{y_2} \frac{1}{r} dy dx \approx \delta \times \int_{x_1}^{x_2} \left( \frac{1}{\delta/2\pi} + \sum_{i=1, n}^{i \neq j} \frac{1}{r_i} \right) dx$$

where  $r = \sqrt{(x-x_j)^2 + (y-y_j)^2}$  and  $\delta = \frac{y_2 - y_1}{n}$

### B. Test Integrations

After integrating over  $\phi$ , two of the  $\mathcal{L}$  operator integrals have a logarithmic singularity. To demonstrate the convergence of this method on such a singularity,  $\log(|x|)$  was numerically integrated on an interval containing zero. Specifically, the function  $(1/2) [\log(|x|) - 1]$  was integrated from -1 to 1 by Gaussian quadrature. The method replaced the zero  $x$  sample by  $\delta/(2\pi)$  or by  $\delta/4$ , where  $\delta$  is the local point spacing. The point spacing varies in Gaussian quadrature but, far from the ends, its local value is approximately the local value of the weight.

The value of this integral is zero [Dwight 1961], so the output is the numerical error. Figure 9 shows the results. With  $2\pi$ , the error is smaller for all numbers of steps used and much smaller for the larger numbers of steps than it is with 4. Though the author is not aware of a mathematical proof, this shows a higher order of convergence. The failure to continue to converge beyond a part in  $10^8$  is probably due to the error in the abscissas and weights. These are calculated by a routine from CICERO that defines constants with precision not much more than this.

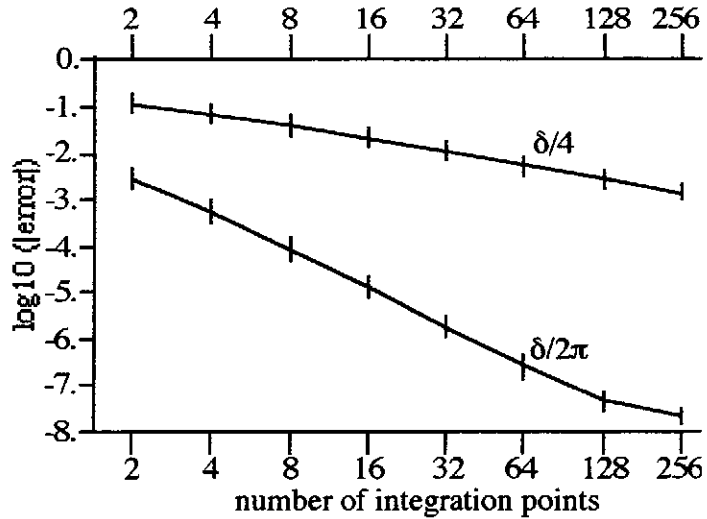


Figure 9: Test Integral of  $(1/2) [\log(|x|) - 1]$

A similar test, done by numerically integrating a function containing  $1/r$  in two dimensions, gave similar results.

### C. Tests in a Boundary Element Method Program

The Figures 10–12 show three comparisons between  $\delta/2\pi$  and  $\delta/4$  for a one meter radius perfectly conducting sphere in a high frequency range, where internal resonances exist. These were done with an LMSC program called KAJRDL. This is again an EFIE calculation. It is sensitive to the numerical integrations, which cause the spurious coupling between inside and outside solutions. The EFIE on a perfect conductor uses only the  $\mathcal{L}$  operator, which is the one that is sensitive to the difference between 4 and  $2\pi$ .

Figure 10 compares calculations done with no subintervals. Figure 11 shows calculations with subintervals only at very short distance. In Figure 12, the distance over which each number of subintervals is used was increased by a factor of ten relative that for Figure 11. The accuracy increases with increasing subintervals. For each figure, over nearly the whole frequency range, the calculations with  $2\pi$  are more accurate than those with 4.

### V. CONCLUSIONS

Each change listed in Part II individually makes modest improvement in the speed to accuracy relation. Together, the improvement is significant for nearly all cases tested and can be striking. All changes, except the subintervals, can be done with little or no increase in complexity. (JRMFOR [Rogers 1990] has another way of varying the number of integration points per basis function.)

In particular,  $\delta/4$  should be changed to  $\delta/(2\pi)$  in the  $\mathcal{L}$  operator of every program that uses this way of dealing with the short range singularity in the  $t$  integration.

### ACKNOWLEDGEMENT

The author thanks Brad Winchester, Chuck Meyers, Kane Yee, Frank Stenger and J. M. Putnam for valuable discussions.

□ KAJRDL 201 Geometry Points  $\delta/(2\pi)$     ○ = 4 KAJRDL 201 Geometry Points  $\delta/4$     △ MIMI Mie Series

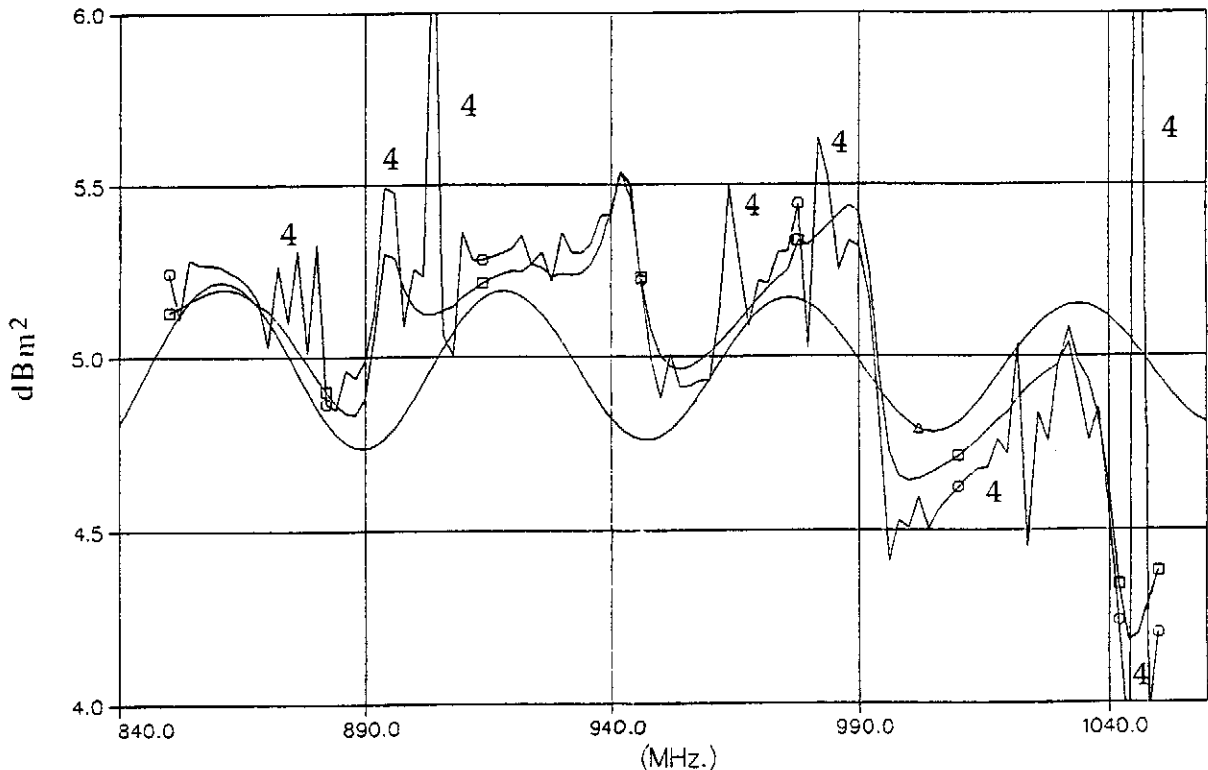


Figure 10: Back-Scatter from a Conducting Sphere, Outer Radius = 1 Meter, No Subintervals

□ KAJRDL 201 Geometry Points  $\delta/(2\pi)$ 
○ KAJRDL 201 Geometry Points  $\delta/4$ 
△ MIMI Mie Series

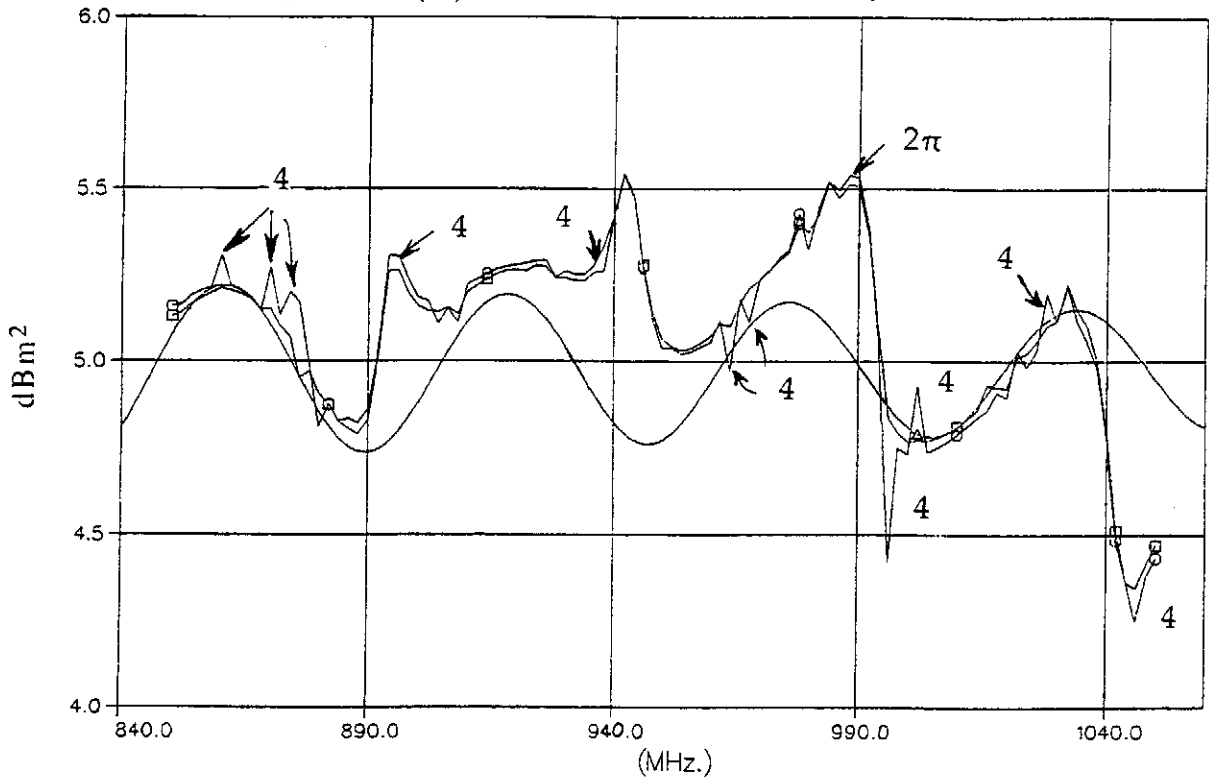


Figure 11: Back-Scatter from a Conducting Sphere, Outer Radius = 1 Meter, Subintervals Used for Very Small  $It-t'$

□ KAJRDL 201 Geometry Points  $\delta/(2\pi)$ 
○ KAJRDL 201 Geometry Points  $\delta/4$ 
△ MIMI Mie Series

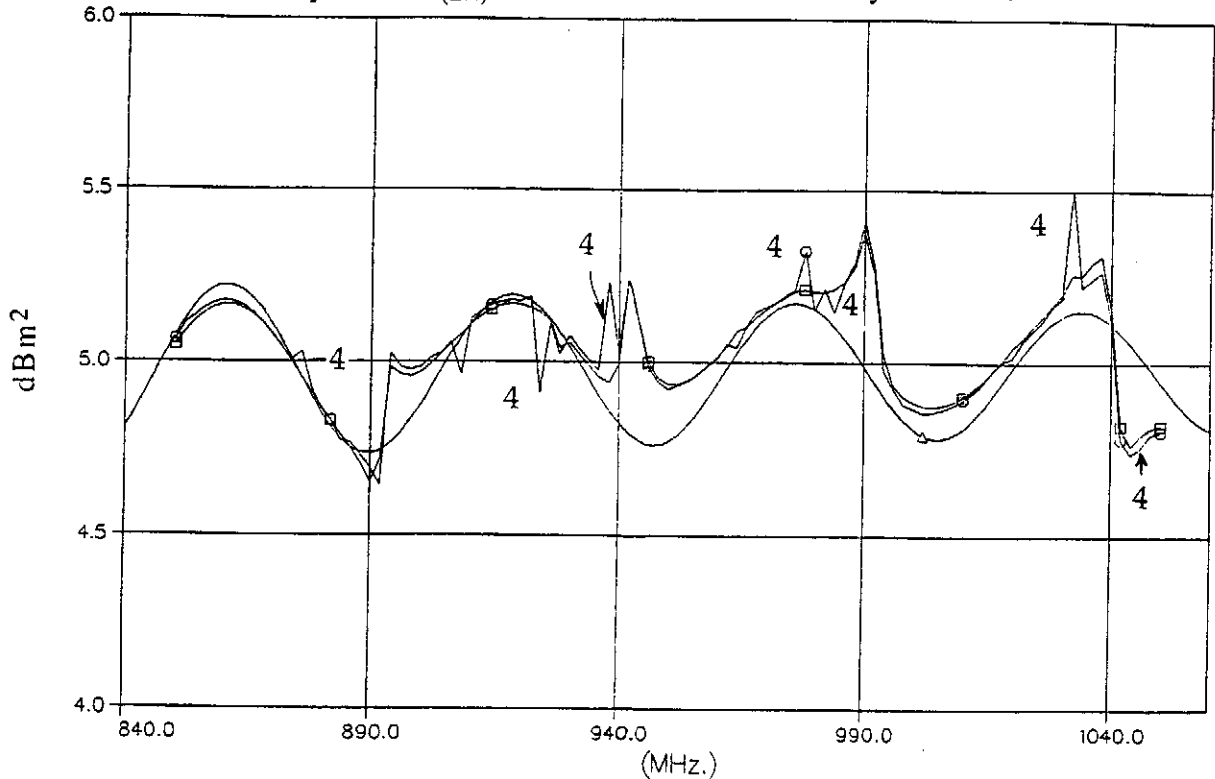


Figure 12: Back-Scatter from a Conducting Sphere, Outer Radius = 1 Meter, Subintervals Used for Longer Distance

## REFERENCES

- Mogens Andreasen and Robert Tanner, "A Wire Grid Lense of Wide Application," *IEEE Trans. Antennas and Propagation*, vol. 10 p. 416-429, 1962 July.
- Herbert Bristol Dwight, *Tables of Integrals and Other Numerical Data*, fourth edition, Macmillan, New York, 1961.
- Allan W. Glisson and Donald R. Wilton, *Simple and Efficient Numerical Techniques for Treating Bodies of Revolution*, University of Mississippi, Engineering Experiment Station, Technical Report No. 105, 129 pp., 1979 March (revised 1982 May).
- Allan Glisson, Donald R. Wilton, "Simple and Efficient Numerical Methods for Problems of Electromagnetic Radiation and Scattering from Surfaces," *IEEE Trans. Antennas and Propagation*, vol. AP-28, p. 593-603, 1980 September.
- P. M. Goggans, A. A. Kishk and A. W. Glisson, "A Systematic Treatment of Conducting and Dielectric Bodies with Arbitrary Thick or Thin Features Using the Method of Moments," *IEEE Trans. Antennas and Propagation*, vol. 40 p. 555-9, 1992 May.
- Srinivasiengar Govind, *Numerical Computation of Electromagnetic Scattering by Inhomogeneous Penetrable Bodies*, dissertation, The University of Mississippi, 1978 December.
- Ahmed A. Kishk "Different Integral Equations for Numerical Solution of Problems Involving Conducting or Dielectric Objects and their Combination," Ph.D. thesis, University of Manitoba, 1986.
- Ahmed A. Kishk and Lotfollah Shafai "Improvement of the Numerical Solution of Dielectric Bodies with High Permittivity," *IEEE Trans. Antennas and Propagation*, vol. AP-37, p. 1486-1490, 1989 November.
- Ahmed A. Kishk, A.W. Glisson and P. M. Goggans, "Scattering from Conductors Coated with Materials of Arbitrary Thickness," *IEEE Trans. Antennas and Propagation*, vol. AP-40, p. 108-112, 1992 January.
- Arthur C. Ludwig, "Wire Grid Modeling of Surfaces," *IEEE Trans. Antennas and Propagation*, vol. AP-35, p. 1045-1048, 1987 September.
- N. Marcuvitz, *Waveguide Handbook*, M.I.T. Radiation Laboratory Series.
- J. R. Mautz and R. F. Harrington, "Radiation and Scattering from Bodies of Revolution," *Applied Scientific Research* vol. 20, p. 405-435, 1969 June.
- Joseph R. Mautz and Roger F. Harrington, *H-Field, E-Field and Combined Field Solutions for Bodies of Revolution*, report number RADC-TR-77-109, Syracuse U., for Hanscom AFB, MA, 1977 March.
- Joseph R. Mautz and Roger F. Harrington, "An improved E-Field Solution for a Conducting Body of Revolution," *Archiv für Elek. und Übertrag.*, Band 36, Heft 5, p. 198-206, 1982 Mai.
- Joseph R. Mautz and Roger F. Harrington, *Application of the New E-Field Solution to a Surface of Revolution*, technical report no. 18, Department of Electrical Engineering, Syracuse University, contract no. N0014-76-C-0225, Office of Naval Research, Syracuse, 1982 December.
- Louis N. Medgyesi-Mitschang and John M. Putnam, "Electromagnetic Scattering from Axially Inhomogeneous Bodies of Revolution," *IEEE Trans. Antennas and Propagation*, vol. AP-32, p. 797-806, 1984 August.
- L. N. Medgyesi-Mitschang, P. L. Huddleston and J. M. Putnam, *Radar Scattering Analysis*, report MDC Q1230, vol. 1-2, McDonnell Douglas Research Laboratories, St. Louis, Missouri, 1984 November.
- John M. Putnam, "CICERO," *The MM/D-BOR(EFIE) General Metal/Dielectric Scattering Code*, McDonnell Douglas Research Labs., 1984.
- J. M. Putnam and L. N. Medgyesi-Mitschang, *Combined Field Formulation for Axially Inhomogeneous Bodies of Revolution (Combined Field Formulation of CICERO)*, MDC report no. QA003, vol. 1-2, McDonnell Douglas Research Laboratories, St. Louis, Missouri, 1987 December.
- James R. Rogers, *Equivalence-Principle/Network Formulations for Aperture Electromagnetics Problems*, Atlantic Aerospace Electronics Corporation, Greenbelt, Maryland, 1989 May.
- James R. Rogers, *JRMBOR: Computation of Scattering from a General Body of Revolution*, technical report JR-2, Atlantic Aerospace Electronics Corporation, Greenbelt, Maryland, 1990 February, revised 1990 July.
- M.E. Smith-Subbarao, *Scattering from a Dielectric Sphere, Mie Solution*, (engineering memorandum), Lockheed Missiles & Space Company, Inc., Palo Alto, Ca., 1987 August 10, and the associated computer program MIE2.
- TCI (TCI International), advertising literature, Sunnyvale, Ca.